Talanta 233 (2021) 122600

Contents lists available at ScienceDirect

Talanta

journal homepage: www.elsevier.com/locate/talanta

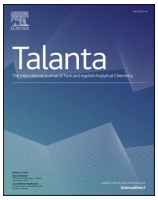

Ultrasensitive electrochemical detection of microRNA based on in-situ catalytic hairpin assembly actuated DNA tetrahedral interfacial probes

Zhangcheng Fu [a], Tong Lv [a], Lili Jiang [a], Chao Xing [b,**], Chunhua Lu [a,*]

[a] MOE Key Laboratory for Analytical Science of Food Safety and Biology, Fujian Provincial Key Laboratory of Analysis and Detection Technology for Food Safety, State Key Laboratory of Photocatalysis on Energy and Environment, College of Chemistry, Fuzhou University, Fuzhou 350116, People's Republic of China
[b] Fujian Key Laboratory of Functional Marine Sensing Materials, Center for Advanced Marine Materials and Smart Sensors, Minjiang University, Fuzhou 350108, People's Republic of China

ARTICLE INFO

Keywords:
Catalytic hairpin assembly
DNA tetrahedral Nanostructure
In-situ
Electrochemical
miRNA detection

ABSTRACT

Selective and sensitive detection of microRNA is crucial for early diagnosis and pathogenesis of disease. Here, we established a novel electrochemical biosensor for simple and accurate analysis of the tumor biomarker microRNA-141, which was based on in-situ catalytic hairpin assembly (CHA) actuated DNA tetrahedral (DTN) interfacial probes. Two hairpin structures used for CHA reaction were placed on the DTN, in which the hairpin H1 on the one vertex of DTN and hairpin H2 embedded in adjacent edge, respective. The target microRNA-141 could open the hairpin H1 and activated the in-situ CHA reaction between H1 and H2 to alter the conformational of DTN, increasing the chances of the direct interaction between methylene blue (MB) and the electrode surface, leading to an increase in the electrochemical signal. Meanwhile, the released miRNA-141 could unfold another H1, enabling the enzyme-free recycling of the target to obtain amplified electrochemical signals. Moreover, the in-situ catalytic hairpin assembly reaction on DTN could shorten the reaction time and enhance the sensitivity. The established biosensor exhibited a wide linear dynamic range of miRNA-141 from 1 fM to 100 pM with a detection limit of 0.32 fM. Besides, the approach can discriminate the target miRNA from mismatched ones with excellent selectivity and can be successfully applied in diluted serum samples, holding great potential for sensitive detection of various biomarkers clinically.

1. Introduction

MicroRNAs (miRNAs) are reported as reliable disease biomarkers for early diagnosis and prognosis of cancers [1–3]. Accurate and sensitive detection of miRNA is particularly desirable to promote the development of diagnosis, prognosis, and therapeutic interventions. However, some crucial issues in miRNAs detection, such as the trace amount, small size and high sequence similarity of miRNA, create problems for miRNA detection. In order to overcoming these difficulty, many sensitive techniques such as fluorescence [4,5], surface plasmon resonance [6–8], electrochemiluminescence [9] and electrochemical DNA sensors [10–15] have been widely utilized. Among these new approaches, electrochemical DNA sensors have garnered considerable attention owing to cost-effectiveness, rapidness and miniaturization. For example, Yang et al. [14] developed an electrochemical sensor for miRNAs detection based on duplex-specific nuclease-assisted target recycling amplifications from different cancer cell lysates. Zhang et al. [15] have demonstrated an electrochemical miRNA biosensing platform using a novel bipedal 2D DNA nanoprobe, which can be used to monitor the different expression of miRNA-21 in MCF-7 cells and HeLa cells. Although acceptable detection sensitivity and specificity were achieved, some inescapable problem also exists, i.e., the unmanageable density and orientation of linear DNA probes on the electrode surface, the requirement of nucleases and signal attenuation strategy. These problems may unavoidably impairs the analytical performance of the electronic DNA sensors [16,17].

Recently, DNA tetrahedral nanostructure (DTN) based electrochemical platforms have received increased attention with the advantages of simple synthesis, excellent mechanical rigidity and structural stability [18–20]. For example, Fan et al. designed a DTN-based electrochemical platform [21,22]. In their design, a capture probe was modified on a DTN at one vertex with three thiol groups at other

* Corresponding author.
** Corresponding author.
E-mail addresses: chaoxing@mju.edu.cn (C. Xing), chunhualu@fzu.edu.cn (C. Lu).

https://doi.org/10.1016/j.talanta.2021.122600
Received 16 February 2021; Received in revised form 4 June 2021; Accepted 6 June 2021
Available online 10 June 2021

vertices, and the DTN was highly ordered and assembled on electrode surfaces, which greatly improves the stability and sensitivity of the electrochemical biosensors. Nevertheless, some inescapable issues still remain to be addressed for DTN based electrochemical platforms. First, the capture probe of many previously reported DTN-based electrochemical methods was designed at the top vertex of DTN, where the distance between the signal molecules blocked by the DTN structure and electrode surface was not close to each other, which influenced the signal output [23]. Second, traditional electrochemical sensors are one-step detection methods without signal-amplification strategies [24], the low detection sensitivity limited further applications. Therefore, establishment of a novel DTN electrochemical probes, which could make signal molecules close to the electrode surface with fantastic amplification efficiency, is highly desirable.

Here, inspired by this demand, we established a novel DNA tetrahedral interfacial probes drived by in-situ catalytic hairpin assembly (CHA) for electrochemical "single on" detection of the tumor biomarker microRNA-141. As an enzyme-free signal amplification approach, CHA could initiate two elaborately designed hairpin DNA to form double strands by toehold-mediated chain replacement mechanism in the present target sequence, which allowing highly sensitive and selective detection of target [25,26]. In our design, the two hairpin structures (methylene blue (MB)-labeled hairpin H1 and hairpin H2) used for CHA reaction were integrated into the one edge and one vertex of the DTN, respectively. In the present of target miRNA, the target could trigger the CHA reaction between the H1 and H2 to form H1/H2 complexes, which will alter the conformational of DTN, increasing the chances of the direct interaction between MB and the electrode surface, thereby accelerating electron transfer, and leading to an amplified electrochemical "single-on" detection of target. Moreover, the in-situ catalytic hairpin assembly reaction by reducing the distance between two reactive hairpin probes on DTN could shorten the reaction time and enhance the sensitivity [27]. Overall, this approach can provide a novel platform for simple, specific, sensitive, and accurate analysis of miRNA in the early stage of cancer.

2. Experimental section

2.1. Reagents and materials

All miRNA and DNA sequences were synthesized from Sangon Biotechnology Company, Ltd. (Table S1). Tris (2-carboxyethy) phosphine hydrochloride (TCEP) and 6-Mercaptohexanol (MCH) were purchased from Sigma (St. Louis, MO, USA). All solutions were prepared with ultrapure water (Milli-Q, 18 MΩ cm resistivity at 25 °C, Merck Millipore) without further purification.

2.2. Non-denaturing polyacrylamide gel electrophoresis (PAGE)

Samples were prepared with DNA-loading buffer (5:1, v/v), and then examined by PAGE in 1 × TBE buffer at 100 V for 60 min with a Bio-Rad imaging system (Hercules, CA), where a 16% polyacrylamide gel were freshly prepared.

2.3. Construction of the biosensor

DTNs were constructed with four single-stranded DNA (S1, S2, S3 and S4) according to previous reports [28]. In brief, equimolar amounts of four strands were mixed with TM buffer (20 mM Tris-HCl and 50 mM $MgCl_2$, pH 8.0), and heated to 95 °C for 5 min and then rapidly cooled to 4 °C to form a stable DTN probe (1 μM). Au electrode was cleaned following the reported protocol.

Prior to the immobilization step, the DTN probe was mixed with TCEP (1 mM) for 1 h to prevent the formation of disulfide bond. Then, the DTN probe was diluted to 0.1 μM with Tris-HCl buffer (20 mM Tris-HCl, 0.2 M NaCl and 5 mM $MgCl_2$, pH 7.4). The 5 μL of DTN probe (0.1 μM) was pipetted on the surface of cleaned AuE and incubated for 2 h to obtain DTN/AuE. The DTN/AuE were subsequently immersed in 2 mM MCH solution to remove the nonspecific DNA adsorption. Afterwards, the probes were washed with PBS buffer and dried with nitrogen, and 5 μL of H1 (1 μM) was dropped onto the DTN/MCH/AuE surface and incubated at 37 °C for 2 h.

2.4. miRNA-141 detection

Five microliters of Tris-HCl buffer with different concentrations of miRNA-141 was applied to the H1/DTN/MCH/AuE. After 90 min of incubation at 37 °C, the H1/DTN/MCH/AuE was rinsed to ensure readiness for the electrochemical measurements.

2.5. Electrochemical measurements

Electrochemical measurements were carried out with a CHI 660D workstation (CH Instruments Inc., Shanghai, China) using a conventional three-electrode configuration consisting of the platinum wire auxiliary electrode, the Ag/AgCl reference electrode and the working AuE (2 mm in diameter). Square wave voltammetry (SWV) was performed in PBS (10 mM) with a step potential of 4 mV, a frequency of 25 Hz, and an amplitude of 25 mV. The electrochemical impedance spectroscopy (EIS) experiments were conducted with 20 mM $[Fe(CN)_6]^{3-/4-}$ containing 1 M KCl with a frequency ranging from 1 to 10^5 Hz and amplitude set at 5 mV.

3. Results and discussion

3.1. Working principle of the biosensor

The working principle of the DTN interfacial probes driven by in-situ CHA was illustrated in Scheme 1. Four single-stranded DNA were first annealed to form a DTN, which acts as the scaffold to form highly ordered orientation as well as spatial isolation. The formed DTN was embedded with a stem-loop hairpin structure (H2) at one of the edges and a capture sequence at the top vertex. Then, the H1 labeled MB can attach to the DTN by the hybridization with capture sequence. Ingeniously, H1 and H2 are designed as fuel chains for CHA reaction, which could be integrated into the nanostructures without sacrificing their functions. The DTN probes with three thiol-modified vertices were immobilized on the surface of AuE via Au–S bond interaction. Without target, H1 would not interact with H2, the signal molecule MB was separated from the electrode surface because of the strong steric hindrance effect of DNA nanostructures, resulting in a weak MB redox current. Whereas, when the target miRNA existed, it would open H1 and then triggered the CHA between H1 and H2 to pull down the strand of H1, enhancing the possibility of direct collision between MB and the electrode surface and accelerating electron transfer. Meanwhile, the target miRNA was released to unfold another H1. As a result, the recycling target could lead to amplified electrochemical signals.

3.2. Verification of DNA assembly amplification

To verify the successful formation of DTN structure after annealing, agarose gel electrophoresis (AGE) and atomic force microscopy (AFM) was performed. As shown in Fig. 1a, lanes 1–4 represent the single-stranded DNA S1, S2, S3 and S4, respectively. The molecular migration rates of DNA combinations formed by two or three strands were in accordance with their molecular weights (lanes 5–14). The band of complete DTN (lane 15) migrated slower than any other combinations due to its increased mass and spatial complexity. AFM images showed a monodisperse cone-shaped DNA tetrahedron structure (Fig. S1). Then, polyacrylamide gel electrophoresis was further employed to confirm CHA amplification strategy. As shown in Fig. 1b, lanes 1 to 4 represented the target miRNA-141, H1 and S1' (the hairpin sequence of H2), and

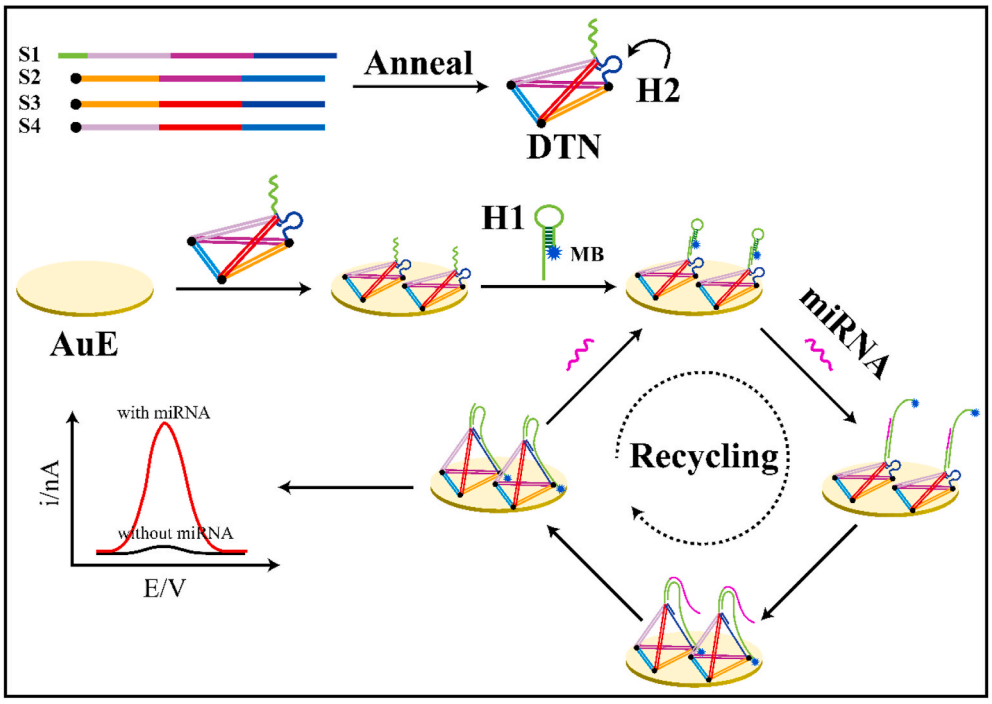

Scheme 1. Scheme of the electrochemical biosensor for miRNA detection based on in-situ CHA actuated DTN interfacial probes.

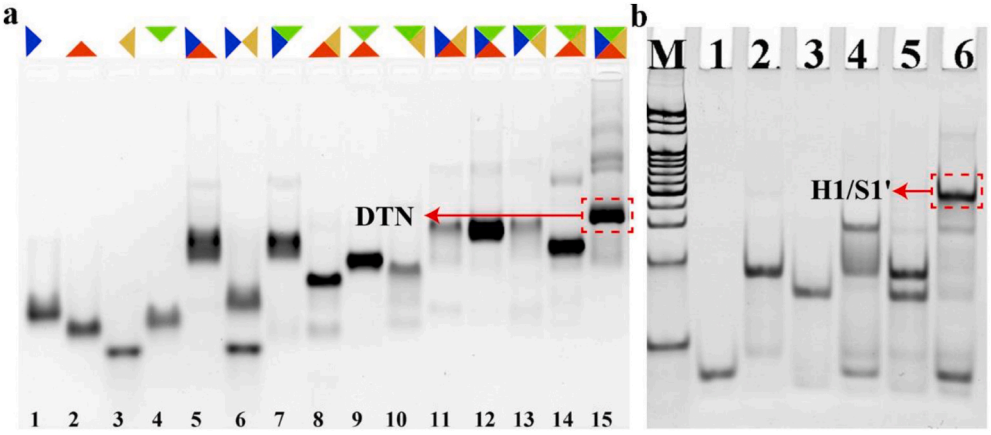

Fig. 1. (a) Analysis of DTN by agarose gel. Blue, red, brown, and green triangles represent S1, S2, S3, and S4, respectively; (b) Polyacrylamide gel electrophoresis analysis of CHA reaction. Lane 1: miRNA-141, lane 2: H1, lane 3: S1', lane 4: miRNA-141+ H1, lane 5:H1+ S1', lane 6: miRNA-141+H1+S1'. The concentrations of DNA strands are 1 μM. (For interpretation of the references to colour in this figure legend, the reader is referred to the Web version of this article.)

miRNA-141+ H1, respectively. Without the miRNA-141, two obvious bands of DNA monomers could be observed in the mixture of H1 and S1' (lane 5). Conversely, a new band with decreased mobility appeared upon the addition of miRNA-141 (lane 6), indicating the feasibility of CHA. The relative distance among probes before and after the microRNA hybridization was characterized using theoretical calculation analysis. As shown in Fig. S2, before the hybridization with miRNA, the relative distance between the MB and electrode surface was 8.91 nm. After the miRNA hybridization, the MB is close to the surface, the relative distance was close to 0 nm. Taken together, these results solidly confirmed the feasibility of the designed in-situ CHA actuated DTN interfacial probes for the amplification detection of target.

3.3. Characterization of the biosensor

The DNA assembled on electrode was characterized by EIS measurement in KCl (1 M) solution containing 20 mM $[Fe(CN)_6]^{3-/4-}$. In Fig. 2, the bare AuE showed a very narrow semicircle (curve a), reflecting its excellent electrical conductivity. Subsequently, when the DTN probes were incubated with the AuE and followed by MCH passivation, the Rct (curves b and c) increased due to the repulsion of the negatively charged DNA and $[Fe(CN)_6]^{3-/4-}$. After assembly of the H1 on the DTN/MCH electrode, an even larger redox current was observed, suggesting that the H1 were successfully immobilized on electrode surface. Upon the addition of the target miRNA-141, the Rct further increased (curve e), demonstrating that the CHA reaction triggered by miRNA-141 could change the configuration of DTN and the enhanced steric hindrance suppressed the electron transfer of $[Fe(CN)_6]^{3-/4-}$. The above results confirmed the developed electrochemical biosensor was successfully constructed.

3.4. Feasibility of the biosensor

To confirm the feasibility of the electrochemical assay for miRNA-

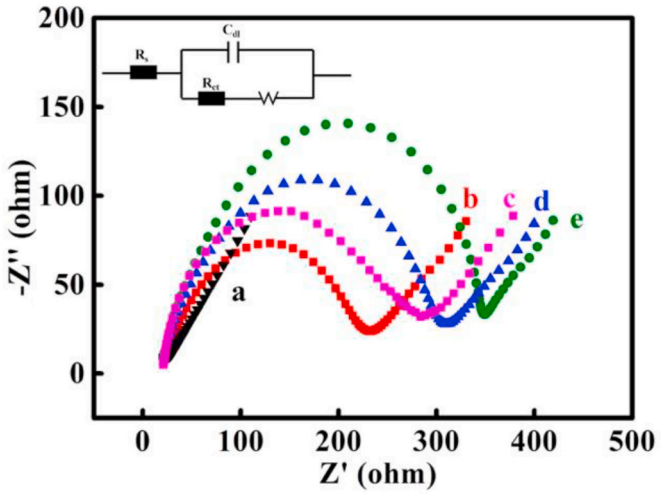

Fig. 2. Characterization of the biosensor with stepwise fabrication based on EIS. (a) bare AuE, (b) DTN/AuE, (c) DTN/MCH/AuE, (D)H1/DTN/MCH/AuE, (E) miRNA-141/H1/DTN/MCH/AuE.

141, SWV measurements were performed on H1/DTN/MCH/AuE. As shown in Fig. 3, when H1/DTN/MCH/AuE was measured with SWV, a weak SWV current response could be observed (curve a), indicating that the signal molecule MB was isolated from the electrode surface, which was attributed to the fact that the large and rigid DNA nanostructures could lead to the strong steric hindrance effect. Once the target miRNA-141 was introduced into the H1/DTN/MCH/AuE, the SWV current response sharply increased (curve b), revealing that miRNA-141 triggered the in-situ CHA process between H1 and H2 to alter the conformational change of DTN, improving the chance of direct interaction between MB and the electrode surface and accelerating electron transfer to obtain amplified electrochemical signals. These results clearly suggested the feasibility of our strategy for miRNA detection.

3.5. Optimization of the experimental conditions

For better performance, experimental conditions including the concentrations of the DTN probe and the CHA reaction times were optimized. In Fig. 4a, the SWV currents enhanced with the DTN concentrations increasing from 0.02 μM to 0.1 μM, and then gradually declined with further increasing of the concentrations of DTN.

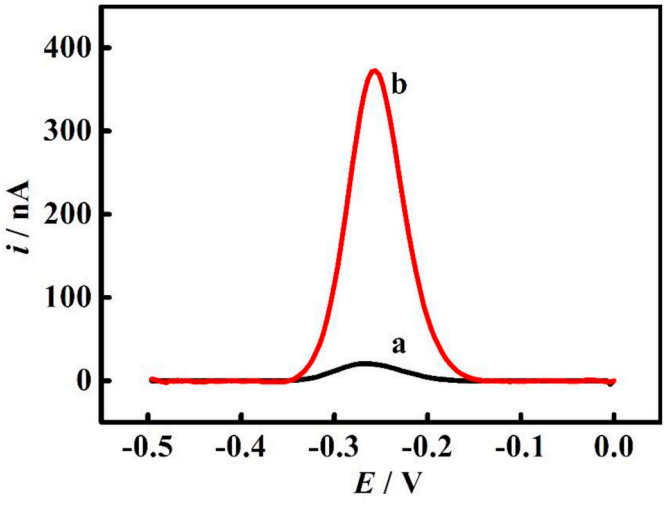

Fig. 3. Feasibility of the biosensor based on SWV. (a) without and (b) with the target miRNA-141.

Accordingly, 0.1 μM DTN was chosen for subsequent experiments. The influence of CHA reaction time was also investigated. As shown in Fig. 4b, the SWV currents enhanced progressively with the CHA reaction times elevating from 10 to 90 min and reached a plateau after 90 min. As a result, 90 min was chosen for the following experiments.

3.6. Analytical performance of the biosensor

After optimizing the experimental conditions, the performance of the biosensor for detecting different concentrations of the target miRNA-141 was evaluated. As shown in Fig. 5a, the SWV current response increased accordingly with the growing concentration of miRNA-141, and a linear relationship was established between the logarithm of the concentration of miRNA-141, and the SWV current response in the range of 1 fM to 100 pM with the equation of i (nA) = 994.2 + 64.08 lgc (M), where $R^2 = 0.9937$. And the limit of detection (LOD) was calculated to be 0.32 fM (LOD = 3σ/S, σ = standard deviation of the blank probe values, S = slope of the calibration curve). Compared with those previously reported methods, the proposed assay exhibited comparable detection performance (Table S2) [29–33].

3.7. Specificity of the biosensor

To explore the specificity of the developed biosensor, a series of commonly coexisting miRNAs including miRNA-155, let-7a miRNA, miRNA-21, miRNA-141 with single base mismatch and three bases mismatches were selected as interfering factors. As shown in Fig. 6, the SWV responses were negligible for interfering miRNA, while the SWV responses of miRNA-141 increased significantly even with a 10-fold lower concentration (100 pM). Moreover, the SWV response of the mixture containing these interfering miRNAs and miRNA-141 (100 pM) was almost similar to that of miRNA-141. Overall, these results demonstrated that the proposed biosensor retained high selectivity.

3.8. Applications of the biosensor in human serum

To further testify the practicality of the proposed biosensor, the target miRNA-141 in human serum samples were determined by the proposed strategy. Recovery rates were calculated by the standard addition method. In Table 1, the recovery rates ranged from 98.4% to 103% with RSD <5.68%, suggesting that the prepared sensor was promising for practical applications in biomedical research and clinic analysis.

4. Conclusions

In summary, an electrochemical biosensor was successfully constructed for ultrasensitive detection of miRNA-141 by using the in-situ CHA reaction actuated DTN interfacial probes. The target miRNA-141 triggered the in-situ CHA reaction on DNA tetrahedral scaffold to alter the conformation of DTN, improving the chance of direct interaction between MB and the electrode surface and accelerating electron transfer for highly sensitive single-on analysis of miRNA. The developed biosensor exhibited desirable sensitivity and specificity for miRNA-141 detection, with a low LOD with 0.32 fM. In addition, this approach was applied for the evaluation of miRNA in serum samples with satisfied results. With these features, the proposed method can be potentially applied for early diagnosis of diseases and biomedical research.

Credit author statement

Zhangcheng Fu is now a master student at the MOE Key Laboratory for Analytical Science of Food Safety and Biology, Fuzhou University, China. Her current research focuses on the construction of nucleic acid-based biosensors and their application in cancer diagnosis.

Tong Lv is now a master student at the MOE Key Laboratory for

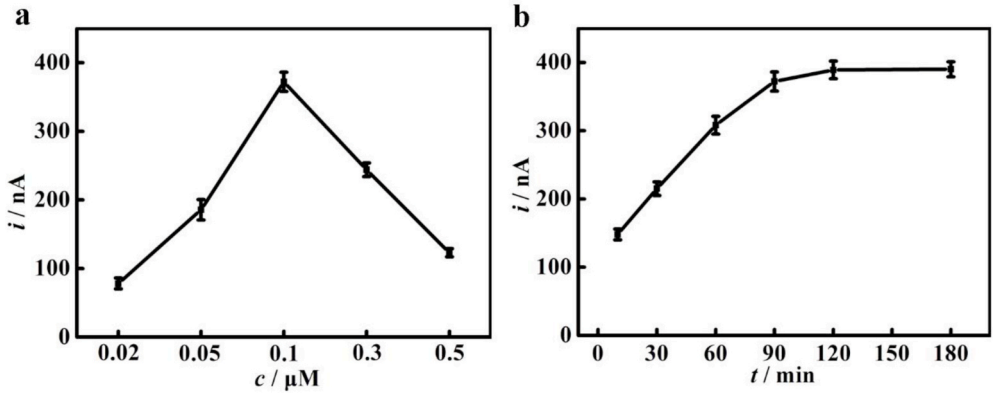

Fig. 4. (a) Effects of DTN concentration on SWV response; (b) Effects of CHA reaction time on SWV response. Error bars, SD, n = 3.

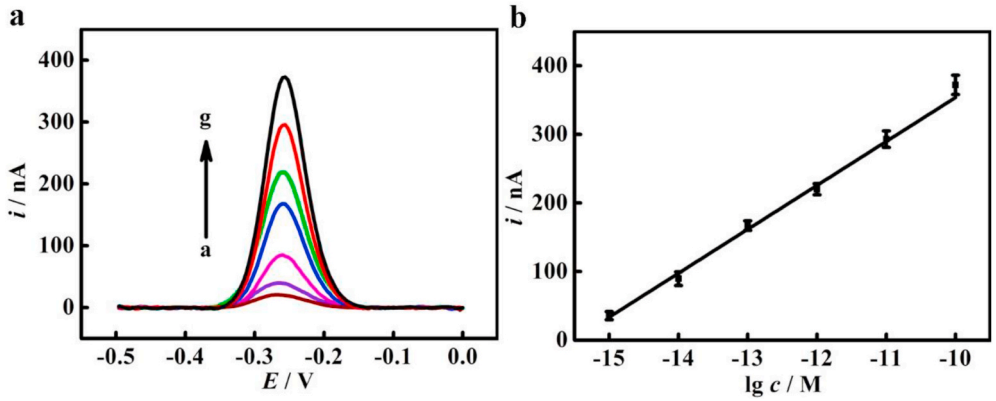

Fig. 5. SWV curves of the present biosensor for detection of different concentrations of miRNA-141 (from a to g: 0, 1 fM, 10 fM, 100 fM, 1 pM, 10 pM, 100 pM); (b) The linear relationship between the corresponding SWV responses and the logarithm of miRNA-141 concentrations. Error bars, SD, n = 3.

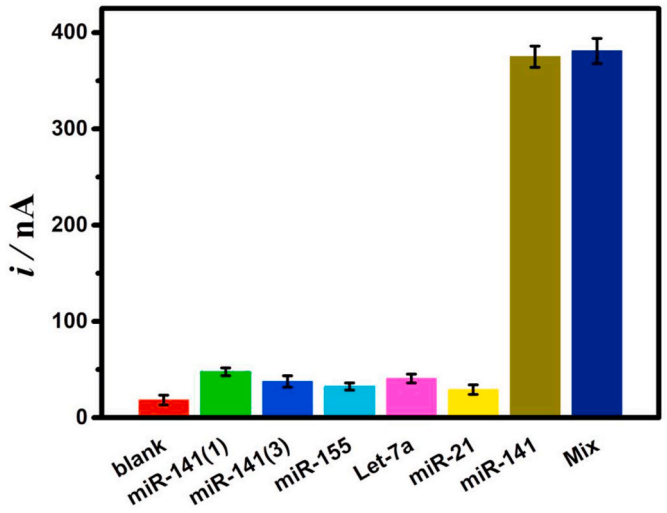

Fig. 6. Specificity of the electrochemical biosensor was analyzed with a blank test, 100 pM single-base mismatched miRNA-141, 100 pM three-base mismatched miRNA-141, 100 pM miRNA-155, 100 pM let-7a, 100 pM miRNA-21, 10 pM miRNA-141, and a mixture of all mentioned miRNAs. Error bars, SD, n = 3.

Table 1
Detection of miRNA-141 in human serum samples (n = 3).

Sample	Added (pM)	Found (pM)	Recovery (%)	RSD (%)
1	0.1 pM	0.103 pM	103.2	4.20
2	1 pM	1.14 pM	114	4.53
3	10 pM	98.4 pM	98.4	5.68

Analytical Science of Food Safety and Biology, Fuzhou University, China. Her current field of research is the construction of nucleic acid-drug and their application in biochemical sensing and cancer treatment.

Lili Jiang received her MS degree from the College of Chemistry, Fuzhou University, China.

Chao Xing received his PhD degree from the College of Chemistry, Fuzhou University, China. He is currently a lecturer at Center for Advanced Marine Materials and Smart Sensors, Minjiang University. His research interests address topics of DNA nanotechnology including DNA machines, DNA sensing and DNA medical engineering.

Chunhua Lu received his BS (2005) and PhD (2011) degrees from College of Chemistry and Chemical Engineering at Fuzhou University (China). From 2011 to 2015, he did his postdoctoral research at The Hebrew University of Jerusalem (Israel) with Prof. Itamar Willner. Dr Chun-Hua Lu is currently a professor in College of Chemistry at Fuzhou University (China). His research interests address topics of DNA nanotechnology, including DNA machines, plasmonic effects using DNA/metal nanoparticle structures, and DNA hydrogels.

Declaration of competing interest

The authors declare that they have no known competing financial interests or personal relationships that could have appeared to influence the work reported in this paper.

Acknowledgements

This research was supported by the National Key R&D Program of China (No. 2018YFA0902600), the National Natural Science Foundation of China (Nos. 21775025, U1705281 and 21974022), the Natural Science Foundation of Fujian (Nos. 2020J06036 and 2020J01861), Fuzhou science and technology project (2020-S-28).

Appendix A. Supplementary data

Supplementary data to this article can be found online at https://doi.org/10.1016/j.talanta.2021.122600.

References

[1] R. Rabieian, M. Boshtam, M. Zareei, S. Kouhpayeh, A. Masoudifar, H. Mirzaei, Plasminogen activator inhibitor type-1 as a regulator of fibrosis, J. Cell. Biochem. 119 (2018) 17–27.
[2] J. Tavakolizadeh, K. Roshanaei, A. Salmaninejad, R. Yari, J. Nahand, H. Sarkarizi, S. Mousavi, R. Salarinia, M. Rahmati, S. Mousavi, R. Mokhtari, H. Mirzaei, MicroRNAs and exosomes in depression: potential diagnostic biomarkers, J. Cell. Biochem. 119 (2018) 3783–3797.
[3] W. Huang, X. Wu, Y. Xue, Y. Zhou, H. Xiang, W. Yang, Y. Wei, MicroRNA-3614 regulates inflammatory response via targeting TRAF6-mediated MAPKs and NF-κB signaling in the epicardial adipose tissue with coronary artery disease, Int. J. Cardiol. (2020).
[4] L. He, D.Q. Lu, H. Liang, S. Xie, C. Luo, M. Hu, L. Xu, X. Zhang, W. Tan, Fluorescence resonance energy transfer-based DNA tetrahedron nanotweezer for highly reliable detection of tumor-related mRNA in living cells, ACS Nano 11 (2017) 4060–4066.
[5] X. Li, D.X. Li, W.J. Zhou, Y.Q. Chai, R. Yuan, Y. Xiang, A micro RNA-activated molecular machine for non-enzymatic target recycling amplification detection of microRNA from cancer cells, Chem. Commun. 51 (2015) 11084–11087.
[6] S. Yudie, L. Tao, Composition-tunable hollow Au/Ag SERS nanoprobes coupled with target-catalyzed hairpin assembly for triple-amplification detection of miRNA, Anal. Chem. 90 (2018) 11614–11621.
[7] X. Wang, W. Lv, J. Wu, H. Li, F. Li, In situ generated nanozyme-initiated cascade reaction for amplified surface plasmon resonance sensing, Chem. Commun. (Camb.) 56 (2020) 4571–4574.
[8] M. Zhu, Z. Sun, Z. Zhang, S. Zhang, Ultrasensitive SERS detection of highly homologous miRNAs by generating 3D organic-nanoclusters and a functionalized chip with locked nucleic acid probes, Chem Commun (Camb) 54 (2018) 13431–13434.
[9] L. Zhu, J. Ye, S. Wang, M. Yan, X. Yang, Dual amplification ratiometric biosensor based on a DNA tetrahedron nanostructure and hybridization chain reaction for the ultrasensitive detection of microRNA-133a, Chem. Commun. 55 (2019) 11551–11554.
[10] P.S. Sfragano, S. Pillozzi, I. Palchetti, Electrochemical and PEC platforms for miRNA and other epigenetic markers of cancer diseases: recent updates, Electrochem. Commun. 124 (2021).
[11] R. Miranda-Castro, I. Palchetti, N. de-los-Santos-Alvarez, The translational potential of electrochemical DNA-based liquid biopsy, Front. Chem. 8 (2020).
[12] F. Bettazzi, S. Laschi, D. Voccia, C. Gellini, G. Pietraperzia, L. Falciola, V. Pifferi, A. Testolin, C. Ingrosso, T. Placido, R. Comparelli, M.L. Curri, I. Palchetti, Ascorbic acid-sensitized Au nanorods-functionalized nanostructured TiO2 transparent electrodes for photoelectrochemical genosensing, Electrochim. Acta 276 (2018) 389–398.
[13] D. Voccia, M. Sosnowska, F. Bettazzi, G. Roscigno, E. Fratini, V. De Franciscis, G. Condorelli, R. Chitta, F. D'Souza, W. Kutner, I. Palchetti, Direct determination of small RNAs using a biotinylated polythiophene impedimetric genosensor, Biosens. Bioelectron. 87 (2017) 1012–1019.
[14] C.Y. Yang, B.T. Dou, K. Shi, Y.Q. Chai, Y. Xiang, R. Yuan, Multiplexed and amplified electronic sensor for the detection of MicroRNAs from cancer cells, Anal. Chem. 86 (2014) 11913–11918.
[15] X. Zhang, Z. Yang, Y. Chang, M. Qing, R. Yuan, Y. Chai, Novel 2D-DNA-nanoprobe-mediated enzyme-free-target-recycling amplification for the ultrasensitive electrochemical detection of MicroRNA, Anal. Chem. 90 (2018) 9538–9544.
[16] G. Peng, X. Li, F. Cui, Q. Qiu, X. Chen, H. Huang, Aflatoxin B1 electrochemical aptasensor based on tetrahedral DNA nanostructures functionalized three dimensionally ordered macroporous MoS2-AuNPs film, ACS Appl. Mater. Interfaces 10 (2018) 17551–17559.
[17] S.C. Jie Wu, Colin Halford, David A. Haake, J. Wang, Ternary surface monolayers for ultrasensitive (zeptomole) amperometric detection of nucleic acid hybridization without signal amplification, Anal. Chem. 82 (2010) 8830–8837.
[18] L. Yang, X. Yin, P. Gai, F. Li, A label-free homogeneous electrochemical cytosensor for the ultrasensitive detection of cancer cells based on multiaptamer-functionalized DNA tetrahedral nanostructures, Chem. Commun. 56 (2020) 3883–3886.
[19] X. Wang, S. Niu, M. Wei, S. Liu, R. Liu, C. Shi, C. Ma, Ultrasensitive electrochemical DNA biosensor based on a tetrahedral structure and proximity-dependent surface hybridization, Analyst 145 (2019) 150–156.
[20] M. Lin, J. Wang, G. Zhou, J. Wang, N. Wu, J. Lu, J. Gao, X. Chen, J. Shi, X. Zuo, C. Fan, Programmable engineering of a biosensing interface with tetrahedral DNA nanostructures for ultrasensitive DNA detection, Angew. Chem. Int. Ed. 54 (2015) 2151–2155.
[21] Z. Ge, M. Lin, P. Wang, H. Pei, J. Yan, J. Shi, Q. Huang, D. He, C. Fan, X. Zuo, Hybridization chain reaction amplification of microRNA detection with a tetrahedral DNA nanostructure-based electrochemical biosensor, Anal. Chem. 86 (2014) 2124–2130.
[22] M.H. Lin, J.J. Wang, G.B. Zhou, J.B. Wang, N. Wu, J.X. Lu, J.M. Gao, X.Q. Chen, J. Y. Shi, X.L. Zuo, C.H. Fan, Programmable engineering of a biosensing interface with tetrahedral DNA nanostructures for ultrasensitive DNA detection, Angew. Chem. Int. Ed. 54 (2015) 2151–2155.
[23] Y. Wen, H. Pei, Y. Shen, J. Xi, M. Lin, N. Lu, X. Shen, J. Li, C. Fan, DNA Nanostructure-based Interfacial engineering for PCR-free ultrasensitive electrochemical analysis of microRNA, Sci. Rep. 2 (2012) 867.
[24] X. Chen, G. Zhou, P. Song, J. Wang, J. Gao, J. Lu, C. Fan, X. Zuo, Ultrasensitive electrochemical detection of prostate-specific antigen by using antibodies anchored on a DNA nanostructural scaffold, Anal. Chem. 86 (2014) 7337–7342.
[25] P. Yin, M.T. Choi, Calvert Harry, R. Colby, Pierce A. Niles, Programming biomolecular self-assembly pathways, Nature 451 (2008) 318–322.
[26] Z.H. Qing, J.L. Hu, J.Y. Xu, Z. Zou, Y.L. Lei, T.P. Qing, R.H. Yang, An intramolecular catalytic hairpin assembly on a DNA tetrahedron for mRNA imaging in living cells: improving reaction kinetics and signal stability, Chem. Sci. 11 (2020) 1985–1990.
[27] Q.M. Wei, J. Huang, J. Li, J.L. Wang, X.H. Yang, J.B. Liu, K.M. Wang, A DNA nanowire based localized catalytic hairpin assembly reaction for microRNA imaging in live cells, Chem. Sci. 9 (2018) 7802–7808.
[28] L. He, D.Q. Lu, H. Liang, S.T. Xie, C. Luo, M.M. Hu, L.J. Xu, X.B. Zhang, W.H. Tan, Fluorescence resonance energy transfer-based DNA tetrahedron nanotweezer for highly reliable detection of tumor-related mRNA in living cells, ACS Nano 11 (2017) 4060–4066.
[29] B. Kou, Y. Chai, Y. Yuan, R. Yuan, Dynamical regulation of enzyme cascade amplification by a regenerated DNA nanotweezer for ultrasensitive electrochemical DNA detection, Anal. Chem. 90 (2018) 10701–10706.
[30] Z. Xu, L. Liao, Y. Chai, H. Wang, R. Yuan, Ultrasensitive electrochemiluminescence biosensor for MicroRNA detection by 3D DNA walking machine based target conversion and distance-controllable signal quenching and enhancing, Anal. Chem. 89 (2017) 8282–8287.
[31] L. Lu, J. Wang, W. Miao, X. Wang, G. Guo, Electrogenerated chemiluminescence biosensor with a tripod probe for the highly sensitive detection of MicroRNA, Anal. Chem. 91 (2019) 1452–1459.
[32] Y. Chang, M. Li, Z. Wu, Y. Zhuo, Y. Chai, Q. Xiao, R. Yuan, Homogeneous entropy catalytic-driven DNA hydrogel as strong signal blocker for highly sensitive electrochemical detection of platelet-derived growth factor, Anal. Chem. 90 (2018) 8241–8247.
[33] S. Bi, S. Yue, W. Song, S. Zhang, A target-initiated DNA network caged on magnetic particles for amplified chemiluminescence resonance energy transfer imaging of microRNA and targeted drug delivery, Chem Commun (Camb) 52 (2016) 12841–12844.